Nonlinear Waves in Randomised Granular Chains

Candidate Number

53904

20th March 2009

Contents

List of Figures

List of Tables

Abstract

Since the seminal research by Fermi, Pasta, and Ulam in the 1950s, chains of nonlinear oscillators have been studied in numerous areas of physics. In this essay, we examine one-dimensional granular lattices, which consist of a chain of beads. Upon striking one end of the chain, a highly nonlinear wave propagates through it. Using experimental and numerical methods, we study the relation between the propagated wave and the properties of the beads used.

Previously, regular arrangements of heterogeneous chains have been studied. One of these arrangements involved chains of 1:1 dimers, where each dimer is a pair of two beads of different materials. We follow on from this work by randomising the orientation of these dimers. Because each dimer has two different orientations, we can consider it as a "spin", and hence consider the lattice as a spin chain.

The main result presented here is the discovery of two different regimes of behaviour of the propagated wave: when many dimers are oriented in the same direction, we obtain "clean" wave propagation where a distinct solitary wave pulse passes through the chain; when many dimers are oriented in different directions, we obtain "delocalisation" where the energy of the wave spreads out across all the beads.

Acknowledgements

I would first of all like to thank my supervisor, Dr. Mason A. Porter, who encouraged and challenged me through the course of the year. His help was invaluable and without it this work would not have come to fruition. Nicholas Boechler supplied me with many wonderful diagrams, some of which are displayed here. Of course, I am thankful to the rest of our collaborators as well – Dr. Laurent R. Ponson, Assoc. Prof. Panayotis G. Kevrekidis, and Asst. Prof. Chiara Daraio.

Next, I thank Athanasios Tsanas for his constructive criticism, and tips with regards to typesetting. I also acknowledge Graham P. Morris, Dr. W. Brian Stewart, and Dr. Zhongmin Qian for their helpful comments.

Financially, my undergraduate studies are wholly funded by the Jardine Foundation, to whom I am very grateful. I should also mention that Exeter College awarded me a grant last summer during an early phase of the research presented here.

1 Introduction

Since the Fermi-Pasta-Ulam (FPU) problem was investigated more than fifty years ago, lattices with nonlinear interactions between particles have attracted significant scientific interest [4]. In the last few years especially, they have been studied in various contexts, such as biophysics [21], optics [14], solid-state physics [26], and atomic physics [17].

One area of particular recent interest is the study of one-dimensional granular chains, which consist of spherical particles colliding elastically with each other. The behaviour of these chains has been scrutinised by the scientific community [23, 27]. The beads in the chain can be made from a wide range of materials, hence allowing the customization of their properties – mass, radius, elastic modulus, Poisson's ratio, etc. Due to this tunability, we can study in great detail the relationship between various aspects of the chain and the response obtained. It also promises a plethora of potential applications in energy absorbing materials [7], sound focusing devices [6] and other such engineering and physical devices.

Recently, heterogenous chains have begun to receive significant attention [23, 27]. In [23] regular arrangements of heterogeneous lattices, such as "dimers" and "trimers", were investigated. In this essay, I describe the subsequent work carried out (by myself, under the supervision of Dr. Porter, and with collaborators) to build on these insights. By randomising the heterogeneities in the chain, we treated the randomised chain as an analogue of a spin system. By doing so, we were able to study the changes in the behaviour of the system as we varied the order of the system.

While this is ostensibly about chains of particles, it is also part of a

broader thrust of research into nonlinear systems. In a 1958 paper [2] Anderson introduced the idea "Anderson Localization" in electromagnetism, and it has since been studied in various areas of phyics. It occurs in linear and weakly nonlinear systems, so here in this strongly nonlinear system we look for an analogous phenomenon, related to recent studies linking Anderson localization and the FPU problem [16]. Learning more about the nature of "nonlinear localisation" would be an important step in understanding disordered systems.

Before plunging into the nature of the research we carried out, I first outline a few key concepts. In the rest of this section, I will discuss solitary waves and the Fermi-Pasta-Ulam problem. I will then present my methodology, results, and conclusions.

1.1 Solitary Waves

In 1834, Scottish naval engineer John Scott Russell observed what he termed a "Wave of Translation" in a barge canal [25]. The theory behind this was initiated in 1895 by Didierik Korteweg and Gustav de Vries in [15] where they investigated an equation modelling shallow water waves, now known as the Korteweg-de Vries (KdV) equation. Much later in 1965, Zabusky and Kruskal discovered solitary wave solutions to the KdV equation [28]. Since then, solitary waves have been used to explain phenomena in many areas of physics, as solutions to various celebrated partial differential equations. A few examples are the nonlinear Schrödinger equation [1], Landau-Lifshitz equation [11], and the sine-Gordon equation [22].

A solitary wave is essentially a packet of energy; however, unlike normal

waves, it does not disperse or suffer attenuation of its amplitude, but remains the same shape. Loosely speaking, this occurs due to the "balancing" of the nonlinearity and dispersion effects in the system. (Dispersion, where waves of different wavelengths travel at different speeds, would normally cause a wave to separate into different components.)

Solitons, a type of solitary wave, have the additional property that a collision with another soliton leaves it unscathed but for a change in phase [10]. Solitons have been one of the main foci of research into solitary waves, and in fact the terms "soliton" and "solitary wave" are often used interchangeably. The study of solitary waves and related objects remains a very active research area.

To construct an example of a solitary wave consider the KdV equation:

$$\phi_t + \phi_{xxx} + \mu^2 \phi \phi_x = 0, \tag{1}$$

where μ is a constant. Because a solitary wave maintains its shape, it must be of the form $\phi(x,t) = f(x \pm ct)$. Consider waves travelling to the right, so $\phi = f(x - ct)$. (The derivation is identical for waves travelling to the left.) Let $y := x - ct$, then Eq. (1) becomes:

$$\begin{aligned} -c\frac{df}{dy} + \frac{d^3 f}{dy^3} + \mu^2 f \frac{df}{dy} &= 0 \\ -cf + \frac{d^2 f}{dy^2} + \frac{\mu^2}{2} f^2 &= A \end{aligned} \tag{2}$$

which can be solved exactly to give

$$f(y) = \frac{3c}{\mu^2} \operatorname{sech}^2 \frac{\sqrt{c}}{2}(y - a), \tag{3}$$

where a is a constant. This gives (see Fig. 1):

$$\phi(x,t) = f(x - ct) = \frac{3c}{\mu^2} \operatorname{sech}^2 \frac{\sqrt{c}}{2}(x - ct - a). \tag{4}$$

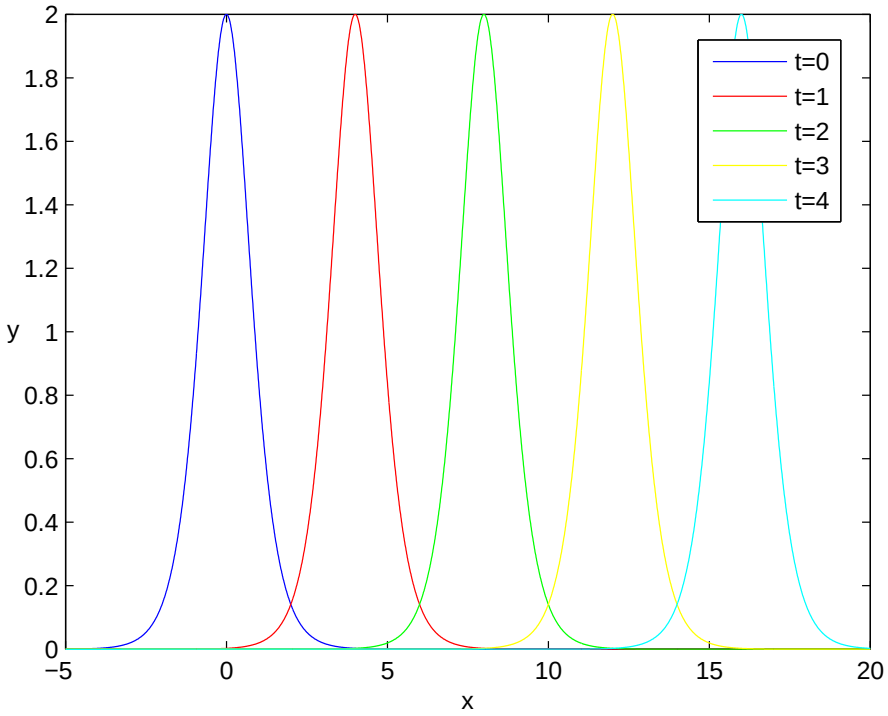

Figure 1: A soliton solution of Eq. (1) – it is described by (4) with $\mu = \sqrt{6}$, $c = 4$, $a = 0$. As time increases it travels to the right and maintains its shape.

In a granular chain, upon striking one end of the chain, a solitary wave is formed which propagates through the chain. These waves have a support of just a few particle sites – an analytical derivation in [23] of solution widths in the continuum limit indicates that for a homogeneous chain, the mean pulse width is only about 5 particles. As such, this system provides one of the most experimentally realisable ways for us to study "compactons", which are solitary waves with compact support [24]. More conventional solitons have infinite, often exponential "tails".

1.2 The Fermi-Pasta-Ulam Problem

While working at Los Alamos National Laboratory under the auspices of the U.S. Atomic Energy Commission, Enrico Fermi, John Pasta, and Stanislaw Ulam, and Mary Tsingou [9] conducted some ground-breaking research on nonlinear systems [12]. Their 1955 report described one of the earliest forays into scientific computation, where they simulated a chain of 64 particles connected by nonlinear springs. In addition to the normal linear spring forces, they added a small nonlinear perturbation – either quadratic, cubic or a piecewise linear approximation of a cubic. A typical equation of motion for the systems they were studying would be:

$$m\frac{d^2x_j}{dt^2} = k(x_{j+1} + x_{j-1} - 2x_j)[1 + \alpha(x_{j+1} - x_{j-1})], \tag{5}$$

where x_j is the displacement of the jth particle from equilibrium, k is the spring constant in Hooke's law, and α is a nonlinear term added [20].

The results were surprising. They had predicted that thermalization would occur, where the energy would eventually distribute itself between all the modes. However, this was not observed – the systems displayed a complex behaviour instead, where a few specific modes would repeatedly "exchange" energy with each other. This apparent paradox has to do with phenomena such as exactly integrable soliton solutions to nonlinear problems, "deterministic chaos" [8], etc; and the study of the FPU problem has prompted much progress in these and related fields.

For one, when we let the number of particles go to infinity, and consider the continuum limit, we can obtain the KdV equation. This was discovered by Zabusky and Kruskal when they were studying the aforementioned soliton

solutions of the KdV equation [28]. I reproduce below a derivation presented in [20]:

We treat the chain of particles as a string. Since a particle of diameter h and mass m corresponds to a segment of string of length h, we let the density of the string $\rho = \frac{m}{h}$. Similarly the elastic modulus $E = kh$. Then we can rewrite the above equation as:

$$\frac{d^2x_j}{dt^2} = \frac{c^2}{h^2}(x_{j+1} + x_{j-1} - 2x_j)[1 + \alpha(x_{j+1} - x_{j-1})] \tag{6}$$

Now we define $u(x,t)$ the displacement of the string at position x and time t. The equation then becomes a PDE:

$$\begin{aligned} u_{tt}(x,t) =& \frac{c^2}{h^2}(u(x+h,t) + u(x-h,t) - 2u(x,t)) \\ & \times [1 + \alpha(u(x+h,t) - u(x-h,t))] \end{aligned} \tag{7}$$

Now we expand $u(x \pm h, t)$ about x to get:

$$u(x+h,t) + u(x-h,t) - 2u(x,t) = h^2 u_{xx}(x,t) + \frac{h^4}{12}u_{xxxx}(x,t) + O(h^6) \tag{8}$$

and

$$1+\alpha(u(x+h,t)-u(x-h,t)) = 1+\alpha(2hu_x(x,t)+\frac{h^3}{3}u_{xxx}(x,t)+O(h^5)). \tag{9}$$

Substitute (8) and (9) into (7):

$$\begin{aligned} u_{tt} &= c^2(u_{xx} + \frac{h^2}{12}u_{xxxx})[1 + \alpha(2hu_x + \frac{h^3}{3}u_{xxx})] + O(h^4) \\ \frac{1}{c^2}u_{tt} - u_{xx} &= \frac{h^2}{12}u_{xxxx} + 2\alpha h u_x u_{xx} + O(h^3) \end{aligned} \tag{10}$$

If the h^2 term is dropped along with the other higher order terms, we get a system that exhibits behaviour qualitatively different from that seen in the FPU chain – see Appendix 2 for more details.

To look for solitary wave solutions of this, we change variables: $\xi = x - ct$, $\tau = \alpha h c t$, $y(\xi, \tau) = u(x, t)$. The equation then becomes:

$$y_{\xi\tau} - \frac{\alpha h}{2} y_{\tau\tau} = -y_\xi y_{\xi\xi} - \frac{h}{24\alpha} y_{\xi\xi\xi\xi} \tag{11}$$

In the continuum limit, as the length of the chain goes to infinity, the particles become infinitesmal elements so $h \to 0$. We assume α scales with h and let $\mu = \lim_{h\to 0} \sqrt{\frac{h}{24\alpha}}$, giving:

$$y_{\xi\tau} + y_\xi y_{\xi\xi} + \mu^2 y_{\xi\xi\xi\xi} = 0 \tag{12}$$

Now substituting $v = y_\xi$ gives us the KdV equation (1):

$$v_\tau + v v_\xi + \mu^2 v_{\xi\xi\xi} = 0$$

The discovery of this relationship by Zabusky and Kruskal has been instrumental in attempting to unravel the mysteries of the FPU problem – the key point being that the solitons in the KdV equation provide part of the explanation for phenomena observed in the FPU system which cause the lack of thermalization. (See [8] for further discussion.)

2 Methodology

The studies described in this essay were concurrently carried out numerically by me in Oxford and experimentally by collaborators in the California Institute of Technology. In the following subsections, I describe the Hertzian contact model we used, the principles used to measure the "order" in a system, the experimental apparatus, and the numerical simulations.

In this essay I often refer to "weakly nonlinear" or "strongly nonlinear" systems. As a short aside, let me attempt to clarify the differences between the two terms. "Weakly nonlinear" systems are those in which the displacement caused by the nonlinear terms is only a small proportion of the displacement caused by the linear terms. For example, in the FPU chain, the nonlinear terms account for less than a tenth of the displacement [12].

On the other hand, in "strongly nonlinear" systems, most of the displacement is caused by the nonlinear term. In this system of particles presented below (13), there is no linear term at all due to the assumption that the particles interact according to the Hertzian contact model. In fact, without a linear term from gravity or precompression, we cannot usefully linearise the system. Precompression refers to having a constant initial compressive force between the particles; chains of particles with significant precompression have been studied [18, 27]. In [23] there was a linear term due to the presence of gravity which was unavoidable because of the vertical alignment of the beads, but in this essay we use a horizontal setup for the experiments (see section 2.3). Gravity and precompression are methods of introducing a linear term to systems like these, and theoretically by adjusting them one would be able to adjust the strength of the nonlinearity in the system [27].

2.1 Hertzian Contact Model

The chain of beads is modelled as a conservative one-dimensional lattice with Hertzian interactions between particles [18, 23, 27]. The Hertz contact law relates the compression of two adjacent beads to the repelling force between them. Using this model, [23] reported good agreement between the numerical simulations and experimental data, and we obtained similar agreement in this study (see section 3). For our N-particle chain, this Hertzian contact law, together with Newton's Second Law, gives us a set of N coupled 2nd order ordinary differential equations (ODEs):

$$\begin{aligned} \frac{d^2 y_j}{dt^2} &= \frac{A_{j-1,j}}{m_j}\delta_j^{3/2} - \frac{A_{j,j+1}}{m_j}\delta_{j+1}^{3/2}, \\ A_{j,j+1} &= \frac{4E_j E_{j+1}\sqrt{\frac{R_j R_{j+1}}{R_j+R_{j+1}}}}{3[E_{j+1}(1-\nu_j^2) + E_j(1-\nu_{j+1}^2)]}, \end{aligned} \tag{13}$$

where $j \in \{1, \ldots, N\}$, y_j is the coordinate of the centre of the jth particle measured from its rest position, $\delta_j \equiv \max\{y_{j+1} - y_j, 0\}$ for $j \in \{2, \ldots, N\}$, $\delta_1 \equiv 0$, $\delta_{N+1} \equiv \max\{y_N, 0\}$, E_j is the elastic modulus of the jth particle, ν_j is its Poisson's ratio, m_j is its mass, and R_j is its radius. The 0th particle represents the striker, and the $(N+1)$st particle represents the wall.

Very loosely, the elastic modulus and Poisson's ratio of an object are measures of how stiff it is. When a force is applied to an object, the elastic modulus is a measure of how much it deforms in the direction of the force, and the Poisson's ratio is a measure of how much it deforms in the direction perpendicular to the force applied [19].

I will explain Eq. (13) briefly. Newton's Second Law gives us, for the jth

bead:

$$m_j \frac{d^2 y_j}{dt^2} = F_{j-1} - F_{j+1},$$

where F_{j-1} is the force exerted on the jth bead by the $(j-1)$st bead, and F_{j+1} the force exerted on the jth bead by the $(j+1)$st bead. The Hertz contact law then specifies the force between beads: $F_{j-1} = A_{j-1,j}\delta_j^{3/2}$ and $F_{j+1} = A_{j,j+1}\delta_{j+1}^{3/2}$. While a full derivation of the Hertz contact law is too lengthy, I give here a brief justification of the 3/2 power law, as in [27]:

Consider two identical beads of radius R and elastic modulus E. They have an approximately circular contact area with radius $\tilde{r}$, so the area is proportional to $\tilde{r}^2$. Then if we let δ be the overlap of the two beads as above, and r a measure of the deformation of the beads, $r \sim \frac{\delta}{\tilde{r}}$.

Then the pressure on each bead $P = Er$. But pressure is the force per unit area, so $P \sim \frac{F}{\tilde{r}^2}$ also, where F is the (Hertzian) force between the beads. So we get:

$$Er \sim \frac{F}{\tilde{r}^2}.$$

Substituting in $r \sim \frac{\delta}{\tilde{r}}$ and rearranging gives:

$$F \sim E\delta\tilde{r}$$

Geometrically (see Fig. 2), $\tilde{r}^2 \approx 2R\delta$, so $\tilde{r} \sim \sqrt{R\delta}$. Hence we get:

$$F \sim ER^{\frac{1}{2}}\delta^{\frac{3}{2}}. \tag{14}$$

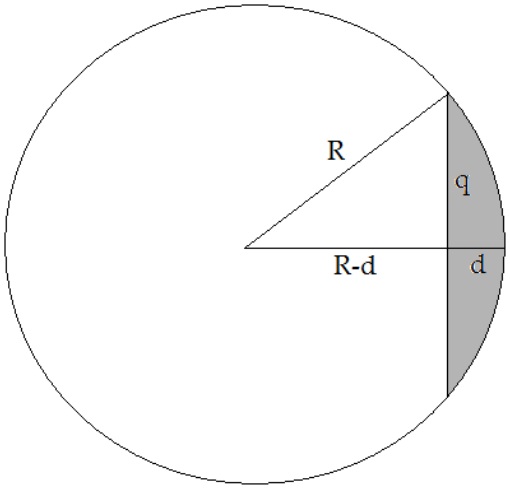

Figure 2: Diagram of deformed bead showing the geometrical step. The grey area is deformed. In the diagram $d = \delta$, $q = \tilde{r}$. The right-angled triangle gives us $\tilde{r}^2 + (R - \delta)^2 = R^2$, and hence $\tilde{r}^2 = 2R\delta - O(\delta^2)$.

2.2 Elastic Spin Systems

Spin, a concept originally associated with the literal spin of subatomic particles, is also used to describe systems in which particles can be in any of several discrete states. It has been used successfully to characterise various phenomena. For example, when studying the magnetic properties of a material, a "spin" would be used to describe the tiny magnetic dipoles in the material, which (in many materials) can be oriented in two directions.

Here it is a convenient quantity used to define the degree of "order" in our chains. In [23] work was done on general classes of dimers and trimers, and a "$N_1 : N_2$ A:B dimer cell" means a "cell" consisting of N_1 particles of material A followed by N_2 particles of material B (see Fig. 3). A similar convention is used for trimers. For most of this essay I will focus on 1:1 dimer cells, that is,

pairs of particles of 2 different materials. As such, because the pair has two possible orientations, we can describe one orientation as an "up" spin and the other as a "down" spin. Now if many of the dimers are oriented in the same way we describe the system as being more ordered, while conversely if fewer dimers are oriented in the same way we decribe the system as being less ordered. So we define an order parameter M as follows:

$$M = \frac{|N_{up} - N_{down}|}{N_{up} + N_{down}} \tag{15}$$

and analogously call this "magnetism".(Henceforth we call "total number of spins" N_{total}, $N_{total} = N_{up} + N_{down}$.) This definition of the order parameter is very simple, and also allows us to vary it easily by flipping any number of dimers one way or another. Also, the definition ensures that M is always between 0 and 1. The crux of the study, therefore, is investigating the behaviour of the propagated wave as this parameter M is varied.

This order parameter is not entirely infallible. For instance, a sequence of spins "up down up down..." would have $M = 0$ but be a regular ordering of tetramer cells. However, as the numerical results are averaged over a large number of simulations, such statistically unlikely outliers do not have consequential effects. A quick calculation reveals that for N_{total} as low as 30, if $M = 0$, the chances of getting a perfect sequence of up spins and down spins (mentioned above), are about 7.8×10^7 to one against. As such, while future work may involve the consideration of such longer-range correlations in measuring order, the quantity M is well-suited for our purposes.

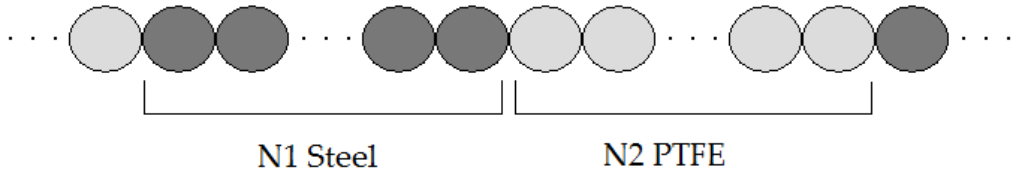

Figure 3: A $N_1 : N_2$ Steel:PTFE dimer cell.

2.3 Experimental Setup

In this study, the experimentalists used 4 different types of beads – large and small steel beads, teflon, and aluminium (see Table 1). They constructed a guide out of two steel bars clamped on a sine plate, and aligned the setup horizontally (see Fig. 4). (A slight tilt – 3.5 degrees – was applied to ensure contact between adjacent particles.) To measure the force and velocity of the propagated waves, specific beads had sensors placed inside them as in [23]. These piezo sensors were inserted into two small steel beads, which were then placed into the chain, one after dimer 19 and one after dimer 23 (see Fig. 4). These sensors measured the force amplitude of the propagated wave at any time. The wave was generated by launching a striker, typically a large steel bead, down a ramp. The initial velocity was then observed with a high-speed camera.

2.4 Numerical Simulations

The method I used for the numerical simulations was to convert the equations of motion into $2N$ coupled 1st order ODEs, which I then solved numerically using the 4th order Runge-Kutta method. (The method is described in Appendix 1.) I then used the same configurations as the experimentalists (see

Table 1: Material properties (mass, Elastic Modulus, Poisson's Ratio, and radius) of the various beads.

Material	m(g)	E (GPa)	ν	Radius (mm)
Large Steel	3.63	193	0.30	4.76
Small Steel	0.45	193	0.30	2.38
PTFE	0.123	1.46	0.46	2.38
Aluminium	1.26	72.4	0.33	4.76

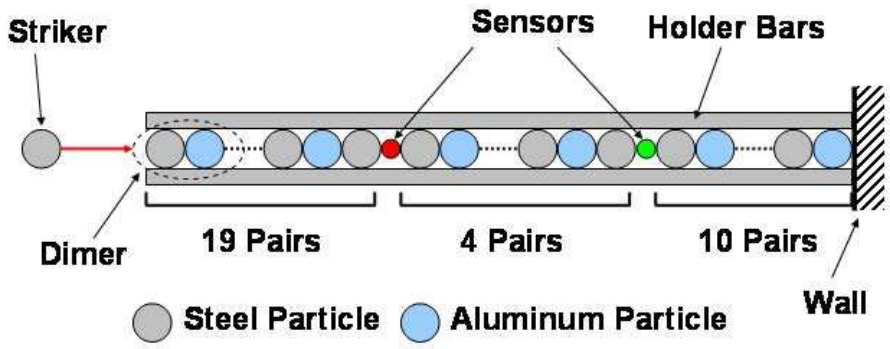

Figure 4: A typical experimental setup. "Pairs" here refer to dimers. Figure courtesy Nicholas Boechler.

the results section below). After confirming that there was agreement between experimental and numerical data, I was able able to use the numerical simulations to carry out various experiments which would have been too difficult or time-consuming to be done in reality.

For one thing, the experimentalists were forced to work with only a few sensors that they had to painstakingly construct themselves, and in this study could only take measurements from two beads in the chain. Even if they had been able to insert a sensor into each bead, doing that would have introduced not insignificant inaccuracies in the material parameters in Table 1. On the other hand, I was able to observe the propagated wave at any bead at any time, and manipulate this data conveniently.

Furthermore, the experiments required large amounts of physical effort, as the chain had to be rearranged manually and carefully set up each time. Another issue was that if a particle is not aligned properly, it undergoes motion in all three spatial dimensions and hence does not adhere to our one-dimensional study. While in [23] the particles were all the same size, one can see that this problem would be exacerbated by having particles of varying radii. The experimentalists used "restraining plates" to combat this, which again had to be reconfigured for each arrangement of dimers. In contrast I was able to automatically conduct numerous simulations in all sorts of different conditions.

In addition, since dissipative effects are not programmed, I was able to observe the nonlinear effects without any obscuration. It turns out that in physical experiments, dissipative effects are often large enough to come into play, especially with "softer" materials such as teflon [23]. A recent paper [5]

studied these effects quantitatively, using similar experimental apparatus. However, this study focuses more on the nonlinear effects. As such, the experimentalists used "harder" materials to minimise dissipation, and I did not include dissipation in my numerical simulations, in order to be able to maintain and examine the propagated wave for any length of chain.

Thus we see that using extensive numerical computations was critical in this study. By its very nature, MATLAB with its vector computations proves to be very useful for handling $2N$ coupled ODEs – it simply treats y as the $2N$-vector required. Essentially, MATLAB provided me with a laboratory with enormous potential. In terms of length of the dimer chain, I was limited only by the computational power of my machine (Intel®Core$^{\text{TM}}$2 Duo 2.40GHz P8600 processor, 4GB RAM) – as a rough estimate, 2000 simulations of a chain with 500 particles took about 2 days to run. (This was the maximum for this study.) One version of the MATLAB code I was using is presented in Appendix 4.

3 Results

First, we look at the results from the experimentalists, and compare them directly with the numerical simulations. They considered a chain of 68 beads – 1 dimer in a fixed orientation, 18 dimers which could be flipped, 14 more "fixed" dimers at the end, and 2 sensors as mentioned in section 2.3 (see Fig. 3). When a wave propagates through a series of dimers with different orientations, we observed that the wave structure can be "disrupted". Hence by having several dimers of fixed orientation, we allow the wave to stabilise somewhat, thus obtaining more accurate measurements.

By considering the first 20 dimers (so $N_{total} = 20$), and changing the orientation of the middle 18 of those 20, they were able to conduct 3 experiments for each value of M (except $M = 1$, which has only one fixed configuration). Note that from the definition of M, for N_{total} even, M can only take the values $\frac{2k}{N_{total}}$, $k = 0, 1, \cdots, \frac{N_{total}}{2}$. So in this case $M = 0, 0.1, 0.2, \cdots, 1$. The two piezo sensors gave two "channels" of data, which were then normalized so that the maximum force in channel 1 was valued 1. Experiments were carried out for both large steel:small steel dimers and large steel:aluminium dimers, but the large steel:small steel results were badly affected by the difficulties with the differing radii (mentioned in section 2.4), so we focus mainly on the large steel:aluminium dimers from now on.

Figure 5 shows some of the experimental results, and the corresponding numerical simulations I carried out. These plots of force against time demonstrate clearly the agreement between the experiments and the numerics. The diagram also shows the solitary wave propagating through the chain – the two peaks are because the graphs from the two sensors are superimposed.

The small differences between the experimental results and the numerics, most noticeably in the secondary waves trailing behind the peaks, is due to dissipation and other inevitable inaccuracies associated with real-world experiments.

We can also look at the maximum force for a specific configuration of M, and then plot a graph of force against M. Figure 6 shows the experimental plot and the numerics, again demonstrating good agreement. Both experiments and numerics indicate the existence of two different "regimes" – a "plateau" where, at low M, the propagated wave does not depend on M; and at higher M, the propagated wave increases with increasing M. From this we postulate a threshold M_c between the two regimes. Having established the agreement between our numerical model and the experimental data, we then proceed to investigate this system more extensively numerically.

I conducted numerical simulations for many values of N_{total}. I would consider a chain of N_{total}+15 dimers, where the last 15 are in fixed orientation. For each value of M I would then run the simulation for 20 randomly chosen configurations of the chain. The maximum force was measured between three and five particles after the end of the flipped dimers. This was then normalised, averaged and plotted – Figure 7 shows diagrams for 32, 64, 128 and 256 dimers. We can see much more clearly now the two regimes and the threshold.

We also note that M_c increases with increasing N_{total}. Hence, for a very long chain of dimers, one would expect that only very few dimers oriented in the "wrong" direction would cause a propagated wave to be in the delocalized regime, which could have possible industrial applications, for instance in

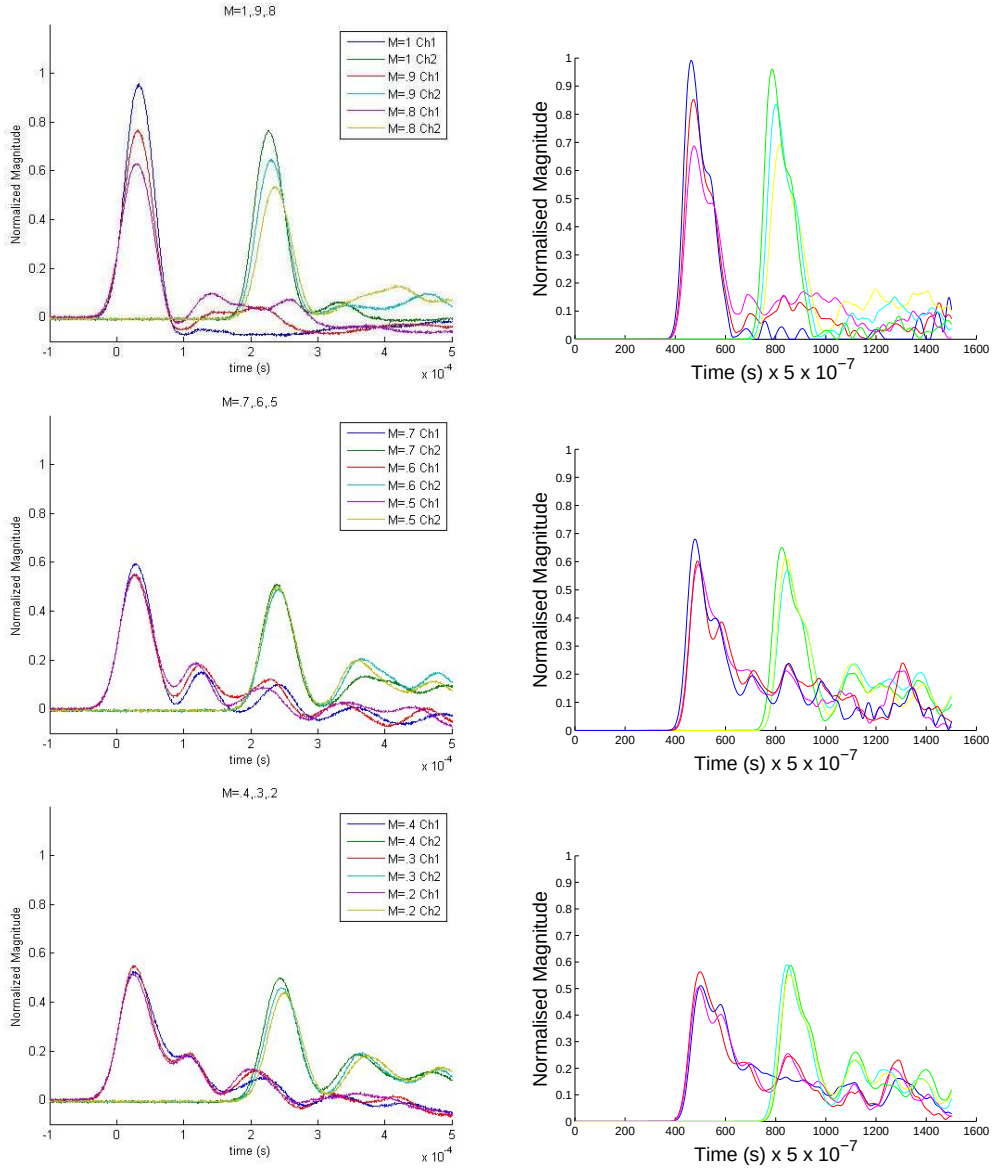

Figure 5: (Left) Experimental plots for steel:aluminium dimers – for high M (top), medium M (middle) and low M (bottom). (Right) The corresponding numerical simulations. All the diagrams on the left are courtesy Nicholas Boechler.

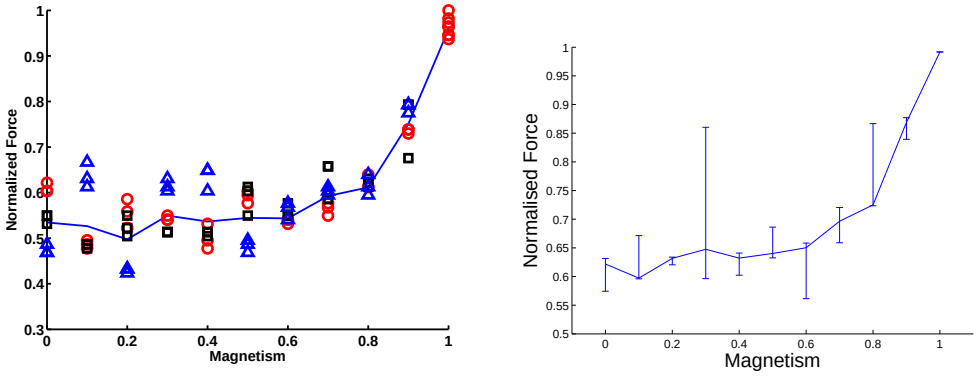

Figure 6: (Left) Experimental plots for steel:aluminium dimers (diagram courtesy Nicholas Boechler). Each colour/shape represents a different configuration (with the same value of M), and each point a separate experimental run. (Right) The numerical simulations corresponding to these runs. There are lines to guide the eye between the median values for each M.

defect detection.

Further research has been carried out on this by collaborators – by applying statistical physics methods to my numerical data, they were able to discover further insights into the behaviour of the wave and the threshold between the two regimes. See Appendix 3 for a brief discussion.

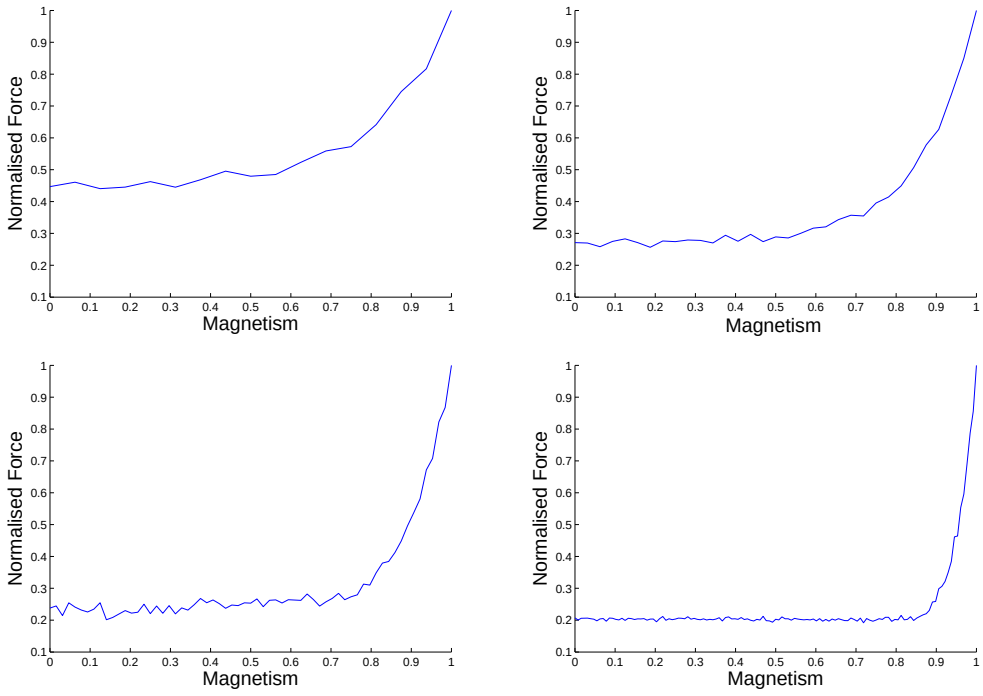

Figure 7: (Top Left) The plot for 32 dimers. (Top Right) 64 dimers. (Bottom Left) 128 dimers. (Bottom Right) 256 dimers.

4 Conclusions and Future Work

In conclusion, we successfully extended previous work done on regular arrangements of heterogenous chains to random arrangements of dimers. By considering each dimer orientation to be either an "up" spin or a "down" spin, we defined an elastic spin chain. My numerical simulations were in good agreement with experiments, motivating us to use more numerical simulations of linear chains to study different aspects of the system in more detail. We discovered a threshold dividing delocalised waves and clean propagation of solitary waves.

From this springboard, much more theoretical work can be done on this system (some of it is described in Appendix 3). This will hopefully allow us to improve our understanding of these heterogeneous configurations. In addition, we also hope to study other more complex systems, such as using trimers for more complicated types of randomisation, and two-dimensional granular crystals on which little work has been done before. Moreover, this and subsequent studies are likely to be useful in certain areas of engineering.

It is hoped that this work will lead to further insights – not just in this field of granular crystals, but also in the broader study of disorder in highly nonlinear systems.

References

[1] Mark J. Ablowitz and Harvey Segur. *Solitons and the Inverse Scattering Transform*. SIAM Studies in Applied Mathematics. Society for Industrial and Applied Mathematics, Philadelphia, Pennsylvania, 1981.

[2] P. W. Anderson. Absence of diffusion in certain random lattices. *Phys. Rev.*, 109(5):1492–1505, 1958.

[3] James E. Broadwell. Shocks and energy dissipation in inviscid fluids: a question posed by Lord Rayleigh. *Journal of Fluid Mechanics*, 347(-1):375–380, 1997.

[4] David K. Campbell, Phillip Rosenau, and George Zaslavsky. Introduction: The Fermi-Pasta-Ulam problem—The first fifty years. *Chaos*, 15(1):015101, 2005.

[5] R. Carretero-González, D. Khatri, Mason A. Porter, P. G. Kevrekidis, and C. Daraio. Dissipative solitary waves in granular crystals. *Physical Review Letters*, 102:024102, 2009.

[6] C. Daraio, V. F. Nesterenko, E. B. Herbold, and S. Jin. Strongly nonlinear waves in a chain of Teflon beads. *Physical Review E*, 72:016603, 2005.

[7] C. Daraio, V. F. Nesterenko, E. B. Herbold, and S. Jin. Energy trapping and shock disintegration in a composite granular medium. *Physical Review Letters*, 96(5):058002, 2006.

[8] T. Dauxois and S. Ruffo. Fermi-Pasta-Ulam nonlinear lattice oscillations. *Scholarpedia*, 3(8):5538, 2008.

[9] Thierry Dauxois. Fermi, Pasta, Ulam and a mysterious lady. *Physics Today*, 61:55–57, 2008.

[10] P. G. Drazin and R. S. Johnson. *Solitons: An Introduction*. Cambridge University Press, 1989.

[11] Ludwig D. Faddeev and Leon A. Takhtajan. *Hamiltonian Methods in the Theory of Solitons*. Springer-Verlag, 1987.

[12] E. Fermi, J. R. Pasta, and S. Ulam. Sudies of nonlinear problems. I. Technical Report Report LA-1940, Los Alamos, 1955.

[13] Joseph Ford. The Fermi-Pasta-Ulam problem: Paradox turns discovery. *Physics Reports*, 213(5):271–310, 1992.

[14] Yuri S. Kivshar and Govind P. Agrawal. *Optical Solitons: From Fibers to Photonic Crystals*. Academic Press, San Diego, California, 2003.

[15] Didierik Korteweg and Gustav de Vries. On the change of form of long waves advancing in a rectangular canal, and on a new type of long stationary waves. *Philosophical Magazine*, 39:422–443, 1895.

[16] V. N. Kuzovkov. The Fermi-Pasta-Ulam paradox, Anderson localization problem and the generalized diffusion approach. arXiv: 0811.1832, 2008.

[17] O. Morsch and M. Oberthaler. Dynamics of Bose-Einstein condensates in optical lattices. *Reviews of Modern Physics*, 78(1):179–215, 2006.

[18] Vitali F. Nesterenko. *Dynamics of Heterogeneous Materials*. Springer-Verlag, New York, NY, 2001.

[19] Lawrence E. Nielsen and Robert F. Landel. *Mechanical Properties of Polymers and Composites*. CRC Press, 1994.

[20] Richard S. Palais. The symmetries of solitons. *Bulletin of the American Mathematical Society*, 34:339–403, 1997.

[21] Michel Peyrard. Nonlinear dynamics and statistical physics of DNA. *Nonlinearity*, 17:R1–R40, 2004.

[22] Andrei D. Polyanin and Valentin F. Zaitsev. *Handbook of Nonlinear PDEs*. Chapman & Hall, 2003.

[23] Mason A. Porter, Chiara Daraio, Ivan Szelengowicz, Eric B. Herbold, and P. G. Kevrekidis. Highly nonlinear solitary waves in heterogeneous periodic granular media. *Physica D*, 238:666–676, 2009.

[24] P. Rosenau and J. M. Hyman. Compactons: Solitons with finite wavelength. *Physical Review Letters*, 70(5):564–567, 1993.

[25] John Scott Russell. Report on waves. In *Fourteenth meeting of the British Association for the Advancement of Science*, 1844.

[26] M. Sato, B. E. Hubbard, and A. J. Sievers. *Colloquium*: Nonlinear energy localization and its manipulation in micromechanical oscillator arrays. *Reviews of Modern Physics*, 78:137, 2006.

[27] Surajit Sen, Jongbae Hong, Edgar Avalos, and Robert Doney. Solitary waves in the granular chain. *Physics Reports*, 462(2):21–66, 2008.

[28] N. J. Zabusky and M. D. Kruskal. Interaction of "solitons" in a collisionless plasma and the recurrence of initial states. *Physical Review Letters*, 15:240–243, 1965.

Appendices

Appendix 1: The 4th-order Runge-Kutta Method

The 4th-order Runge-Kutta method is as follows: Given an initial-value problem of the form

$$\frac{dy}{dx} = f(x, y), \quad y(x_0) = y_0,$$

the method is given by:

$$y_{n+1} = y_n + \frac{j}{6}(k_1 + k_2 + k_3 + k_4),$$

where j is the mesh size so that $x_{n+1} = x_n + j$ and the k's are calculated at each step, thusly:

$$\begin{aligned} k_1 &= f(x_n, y_n) \\ k_2 &= f(x_n + \frac{j}{2}, y_n + \frac{j}{2}k_1) \\ k_3 &= f(x_n + \frac{j}{2}, y_n + \frac{j}{2}k_2) \\ k_4 &= f(x_n + j, y_n + jk_3). \end{aligned}$$

Appendix 2: A Brief Look at $u_{tt} = c^2 u_{xx}(1 + \epsilon u_x)$

From Eq. (10), if we omit h^2 and higher powers of h, we obtain:

$$\frac{1}{c^2} u_{tt} - u_{xx} = 2\alpha h u_x u_{xx}.$$

Because we let $h \to 0$ we can now write the equation as

$$u_{tt} = c^2 u_{xx}(1 + \epsilon u_x),$$

where ϵ is small and positive. This can now be compared to a normal wave equation, but with wave speed dependent on u_x. Typically, this will result in a propagated wave becoming more and more asymmetric until it develops a shock front [13]. (A very rough diagram is shown in Fig. 8.) This type of equation is of significant mathematical interest and has been studied since the 19th century [3, 20].

In any case, the FPU system we want to study here exhibits very different behaviour, in particular near-recurrence to the initial state [12, 20], so this model is not appropriate. In fact, it was a significant discovery for Zabusky and Kruskal when they kept the h^2 term, and subsequently linked the FPU chain to the KdV equation.

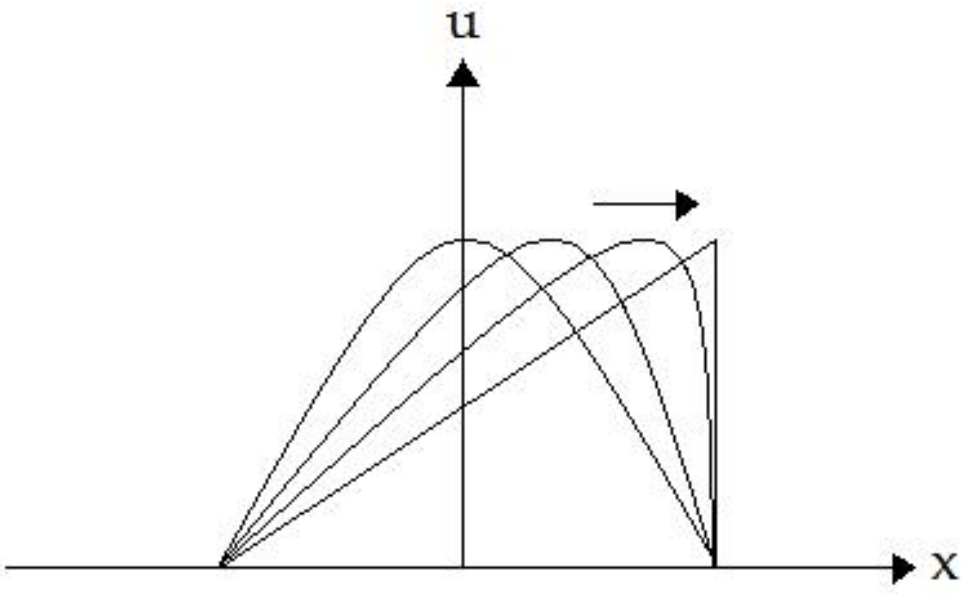

Figure 8: A shock wave occurring as described above. The arrow to the right indicates increasing time.

Appendix 3: Further Insights

Using numerical data I supplied, Laurent Ponson was able to study the behaviour of the propagated wave in greater detail. I present a few of his conclusions below. (The following was based on numerical simulations of a steel:aluminium chain with $N_{total} = 50$, for which $M_c \approx 0.60$.)

In the low-disorder regime, where $M \gg M_c$, we observed a nonlinear wave pulse with width and velocity similar to those observed in regular arrangements of heterogeneous chains [23]. The amplitude of the wave decays exponentially as the wave propagates through the chain:

$$F = e^{-\frac{x_s}{\gamma}},$$

where F is the amplitude of the wave, x_s the sth particle is where the peak of the wave is, and γ a constant depending on the material properties of the chain and the magnetisation M.

Since most of the dimers are oriented in the same way in this regime, we can consider a dimer in the opposite direction to be a "defect". By considering the effect of a single defect on the propagated wave, we can deduce the observed exponential decay. Each defect removes a small fraction of the energy of the wave by $E_{after} = TE_{before}$, where E_{after} is the energy of the wave after the defect, E_{before} the energy of the wave before the defect, and T a transmission coefficient depending on the material properties of the chain. This formula remains accurate in the regime even when multiple defects are next to each other. Now for a chain with magnetisation M, the expected number of defects after passing through x_s particles is $x_s(1 - M)$,

which tells us that the energy of the pulse

$$E = E_0 T^{x_s(1-M)},$$

where E_0 is the initial energy. Now applying the relation $E \sim F^{\frac{5}{3}}$ from [18], which relates the energy of a wave to its amplitude, we regain from before

$$F = e^{-\frac{x_s}{\gamma}}.$$

In the high-disorder regime ($M \ll M_c$), the delocalised wave does not have an obvious "peak" – but by considering the energy at the front of the wave, we were able to observe a similar exponential decay. However, unlike in the low-disorder regime, this does not depend on M – the behaviour of the wave remains qualitatively similar for all M in this regime.

Appendix 4: Sample MATLAB Code

Below I append one version of the MATLAB code I used in this project. This particular version allows one to input a specific configuration of dimers in 0's and 1's, and will return a large matrix with all the values of the force of the wave at any bead at any time.

```
flip=[0 1 0 1 0 1 0 1 0 1 0 1 0 1 0 1 0 1 0 1];
[M,N]=size(flip);
buffer=10;

% number of sites
%ns=6*nf+51; % bead 1 = striker, beads 2--(ns) are the actual beads,
%bead (ns+1) is the wall
ns=2*N+1+buffer;

% time increment
kkmax=30000;

%%%%%%%%%% masses (in kg) %%%%%%%%%%
mass = zeros(1,ns);   % initialize mass vector

m1 = .00045;    % steel
m2 = .000123;  % ptfe (teflon)
m7 = .00360187;   % big steel
m8 = .00126;     %aluminium
```

```
mass(1) = m7;   % steel striker
mass(2:ns) = m7;

%%%%%%%%% young moduli (in PA) %%%%%%%%%
ee = zeros(1,ns);
e1 = 1.93*10^11;
e2 = 1.46*10^9;
e8 = 7.24*10^10;
e7 = e1;

ee(1) = e1;
ee(2:ns) = e1;

%%%%%%%%% poisson ratios (0.1--1); %%%%%%%%%
nunu = zeros(1,ns);

nu1=0.3;
nu2=0.46;
nu8 = 0.33;
nu7 = nu1;

nunu(1)=nu1;
nunu(2:ns)=nu1;

%%%%%%%%% radii %%%%%%%%%
```

```
rr = zeros(1,ns);

r1=.00476/2;
r7=.00952/2;

rr(1:ns)=r7;

%%%%%%%%%% dimer flips %%%%%%%%%%

          for i=1:N
              if flip(1,i)==1
                 mass(2*i)=m7;
                 ee(2*i)=e7;
                 nunu(2*i)=nu7;
                 mass(2*i+1)=m8;
                 ee(2*i+1)=e8;
                 nunu(2*i+1)=nu8;
              else mass(2*i)=m8;
                 ee(2*i)=e8;
                 nunu(2*i)=nu8;
                 mass(2*i+1)=m7;
                 ee(2*i+1)=e7;
                 nunu(2*i+1)=nu7;
                 end
          end
```

```
% force coefficients
alp = zeros(1,ns);

%alp(1) = (4*ee(1)*ee(2)*sqrt(radius(2)))/(3*ee(2)*(1-nunu(1)^2)
          + 3*ee(1)*(1-nunu(2)^2));
alp(1:(ns-1)) = 4*sqrt(rr(1:(ns-1)).*rr(2:ns)
                ./(rr(1:(ns-1))+rr(2:ns))).*ee(1:(ns-1)).*ee(2:ns)
                ./(3*ee(2:ns).*(1-nunu(1:(ns-1)).^2)+3*ee(1:(ns-1))
                .*(1-nunu(2:ns).^2));

ee(ns+1) = 9.02 * 10^10; nunu(ns+1) = 0.34;   % brass
alp(ns) = (4*ee(ns)*ee(ns+1)*sqrt(rr(ns)))/(3*ee(ns+1)*(1-nunu(ns)^2)
           + 3*ee(ns)*(1-nunu(ns+1)^2));   % particle + brass wall

% particle (ns+1) is a brass wall; it has radius(ns+1) = infinity,
% E(ns+1) = 9.02 * 10^10 , and nu(ns+1) = .34

dt=10^-7;

kk=1;
it=1;

u1=zeros(1,ns); pu1=zeros(1,ns);
u=zeros(1,ns); pu=zeros(1,ns);
```

```
apu=zeros(1,ns); k1pu=zeros(1,ns);
k2pu=zeros(1,ns); k3pu=zeros(1,ns);
k4pu=zeros(1,ns);
pu1(1) = 0.443;

timesteps = (kkmax/5)-1;
force = zeros(ns-1,timesteps);

%%%%%%%%% the actual dynamical equations of motion %%%%%%%%%

while (kk < kkmax)
        u=u1; pu=pu1;
        k1u=dt*pu;

        delta(1) = 0;
        delta(2:ns) = max(0,u(1:(ns-1)) - u(2:ns));
        delta(ns+1) = max(0,u(ns) - 0);
        delplot=delta;

        k1pu(1) = dt*(-(alp(1))*delta(2)^(3/2)/mass(1));
        k1pu(2:ns) = dt*((alp(1:(ns-1))).*delta(2:ns).^(3/2)./mass(2:ns)
                    - (alp(2:ns)).*delta(3:(ns+1)).^(3/2)./mass(2:ns));

au=u+k1u/2;
apu=pu+k1pu/2;
```

```
        k2u=dt*apu;

        delta(1) = 0;
        delta(2:ns) = max(0,au(1:(ns-1)) - au(2:ns));
        delta(ns+1) = max(0,au(ns) - 0);

        k2pu(1) = dt*(-(alp(1))*delta(2)^(3/2)/mass(1));
        k2pu(2:ns) = dt*((alp(1:(ns-1))).*delta(2:ns).^(3/2)./mass(2:ns)
                    - (alp(2:ns)).*delta(3:(ns+1)).^(3/2)./mass(2:ns));

au=u+k2u/2;
apu=pu+k2pu/2;

        k3u=dt*apu;

        delta(1) = 0;
        delta(2:ns) = max(0,au(1:(ns-1)) - au(2:ns));
        delta(ns+1) = max(0,au(ns) - 0);

        k3pu(1) = dt*(-(alp(1))*delta(2)^(3/2)/mass(1));
        k3pu(2:ns) = dt*((alp(1:(ns-1))).*delta(2:ns).^(3/2)./mass(2:ns)
                    - (alp(2:ns)).*delta(3:(ns+1)).^(3/2)./mass(2:ns));

au=u+k3u;
```

```
apu=pu+k3pu;

        k4u=dt*apu;

        delta(1) = 0;
        delta(2:ns) = max(0,au(1:(ns-1)) - au(2:ns));
        delta(ns+1) = max(0,au(ns) - 0);

        k4pu(1) = dt*(-(alp(1))*delta(2)^(3/2)/mass(1));
        k4pu(2:ns) = dt*((alp(1:(ns-1))).*delta(2:ns).^(3/2)./mass(2:ns)
                    - (alp(2:ns)).*delta(3:(ns+1)).^(3/2)./mass(2:ns));

u1=u+(k1u+2*k2u+2*k3u+k4u)/6;
pu1=pu+(k1pu+2*k2pu+2*k3pu+k4pu)/6;

     if (mod(kk,5)==0)
        force(1:ns-1,it) = .5*(alp(1:ns-1).*delplot(2:ns).^(3/2)
                           + alp(2:ns).*delplot(3:ns+1).^(3/2));
        it=it+1;
     end;
        kk=kk+1;
end;

imagesc(force)
```